

Theory of Orbital Pumping

Seungyun Han^{**},¹ Hye-Won Ko^{**},² Jung Hyun Oh,² Hyun-Woo Lee,^{1,*} Kyung-Jin Lee,^{2,†} and Kyoung-Whan Kim^{3,‡}

¹Department of Physics, Pohang University of Science and Technology, Pohang 37673, Korea

²Department of Physics, Korea Advanced Institute of Science and Technology, Daejeon 34141, Korea

³Center for Spintronics, Korea Institute of Science and Technology, Seoul 02792, Korea

We develop a theory of orbital pumping, which corresponds to the emission of orbital currents from orbital dynamics. This phenomenon exhibits two distinct characteristics compared to spin pumping. Firstly, while spin pumping generates solely spin (angular momentum) currents, orbital pumping yields both orbital angular momentum currents and orbital angular position currents. Secondly, lattice vibrations induce orbital dynamics and associated orbital pumping as the orbital angular position is directly coupled to the lattice. These pumped orbital currents can be detected as transverse electric voltages via the inverse orbital(-torsion) Hall effect, stemming from orbital textures. Our work proposes a new avenue for generating orbital currents and provides a broader understanding of angular momentum dynamics encompassing spin, orbital, and phonon.

Introduction.— Orbital transport in solids has recently attracted considerable theoretical and experimental interest because nonequilibrium orbital quantities arise from strong crystal field coupling rather than weak spin-orbit coupling (SOC) [1]. It results in intriguing phenomena associated with orbital angular momentum (OAM), including the orbital Hall effect [2–11] and orbital magnetoresistance [12, 13]. In the presence of SOC, these OAM-related phenomena are intimately connected to spin-related ones; the spin Hall effect [14, 15] and spin magnetoresistance [16]. Moreover, analogous to spin torque, which arises from spin injection into a ferromagnet [17, 18], the injection of OAM into a ferromagnet results in orbital torque [19–24] contributing to the net magnetic torque. These findings underscore the electron’s orbital as an essential degree of freedom for understanding angular momentum transport in solids and realizing novel orbitronic devices.

Despite its importance, identifying orbital transport presents challenges because OAM shares the same symmetry operations with spin. Symmetry-wise, distinguishing OAM from spin is thus impossible. Consequently, previous experiments have relied on the quantitative difference between spin Hall and orbital Hall conductivities to identify the orbital physics [11, 13, 21–24]. While the spin Hall conductivity is significant only in a limited number of materials, the orbital Hall conductivity is large in a broad range of materials and often surpasses the maximum value of spin Hall conductivity [8, 25].

Although these quantitative differences are valuable, qualitative differences between the orbital and spin properties are crucial for understanding orbital physics and its unambiguous identification. In this regard, orbital angular position (OAP), which describes different aspects of orbital states from OAM [26], emerges as a crucial element for such qualitative distinctions. It is noted that three OAM operators (L_x, L_y, L_z) are insufficient to completely describe orbital states and additional OAP operators, composed of even-order symmetrized products of L , are essential. Physically, OAP operators capture real orbital states with zero OAM expectation value, such as p_x and p_y orbitals, and mediate the orbital-lattice (i.e., crystal field) coupling [26]. Unlike OAM, which bears analogies to

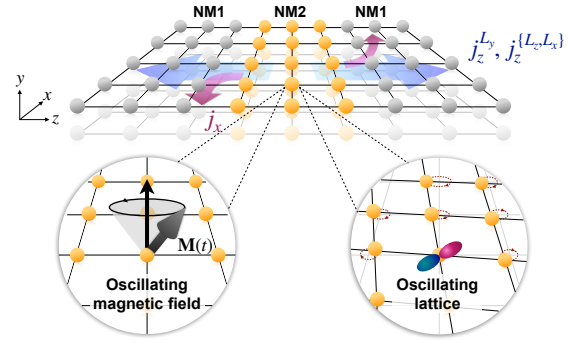


FIG. 1. Schematic illustration of orbital pumping in a model system, NM1/NM2/NM1 (NM = normal metal), driven by an oscillating magnetic field or vibrating lattice. For the magnetic-field-driven case, NM2 may be considered a ferromagnet. j_z^L is an orbital current flowing along z with orbital l , and j_x is a charge current flowing along x .

spin in various aspects, OAP notably lacks a spin counterpart.

Adiabatic pumping [27] provides critical insights into the dynamics of physical systems [28]. For spin dynamics, adiabatic spin pumping has elucidated phenomena such as enhanced magnetic damping [29] and spin motive force [30–34], and served as an efficient means for generating pure spin currents [35, 36]. Spin pumping is connected with spin torque through the Onsager reciprocity [37]. Given orbital torque [19–24], the Onsager reciprocity also guarantees the presence of orbital pumping. Recent studies have investigated orbital pumping [38–40], focusing on OAM pumping but neglecting the contribution of OAP. Therefore, a complete description of orbital pumping is yet to be established.

In this Letter, we present a theory of orbital pumping that incorporates the entire orbital degrees of freedom, encompassing both OAM and OAP. We consider two distinct types of adiabatic orbital pumping. The first type involves the OAM dynamics induced by an AC magnetic field (Fig. 1), similar to the approach used for spin pumping with ferromagnet/normal metal bilayers. The second type, which does not require a ferromagnet, arises from the lattice dynamics, which is realized by applying AC stress to a nonmagnet (Fig. 1). Resulting

AC strain gives rise to orbital pumping through strong orbital-lattice coupling mediated by OAP. We show that both methods generate not only OAM pumping but also OAP pumping. The latter pumping has no spin counterpart and causes an even-order harmonic AC transverse voltage, which is absent for spin pumping and thus allows for unambiguous identification of orbital pumping in experiments.

Orbital pumping by oscillating magnetic field.—For the first type, we examine orbital pumping arising from the dynamics of the orbital moment (i.e., OAM) driven by an AC magnetic field. We ignore the spin degree of freedom to focus solely on orbital responses and neglect SOC for the same reason. To get a tractable analytic formula, we consider a p -orbital system as a minimal model and assume an ideal case where three p -orbitals are degenerate in equilibrium. This ideal case reveals critical qualitative differences between orbital pumping and spin pumping. However, this ideal case is not realized in real materials since p -orbitals are split due to crystal fields. We consider the crystal field effects on orbital pumping in numerical calculations below and demonstrate that the predictions from the ideal case persist in real situations.

We construct a model system of NM1/NM2/NM1 structure (Fig. 1; NM = normal metal) and derive orbital pumping currents induced by time-dependent perturbations to NM2. The perturbation Hamiltonian is $\mathcal{H}(t) = J_{\text{ex}} \mathbf{L} \cdot \mathbf{M}(t)$, where $\mathbf{M}(t)$ is the unit vector of time-dependent magnetic field, J_{ex} is the coupling strength, and \mathbf{L} is the (dimensionless) OAM operator, which is a 3×3 matrix in p -orbital space.

For a degenerate p -orbital system, the orbital is conserved, and the 3×3 Green's function is given by,

$$g = g_0 I + \frac{g_1 - g_{-1}}{2} \mathbf{L} \cdot \mathbf{M}(t) + \frac{g_1 + g_{-1} - 2g_0}{2} [\mathbf{L} \cdot \mathbf{M}(t)]^2, \quad (1)$$

where g_m is the Green's function associated with an eigenstate having an eigenvalue m ($= -1, 0, 1$) of $\mathbf{L} \cdot \mathbf{M}(t)$ and g includes a term quadratic in \mathbf{L} (i.e., OAP). We abbreviate the explicit position dependence of g_m for simplicity. Employing the method developed in Ref. [34], we compute the 3×3 matrix pumped current density operator j_α where α is the flow direction:

$$j_\alpha / (-e) = \mathbf{j}_\alpha^{\text{OAM}} \cdot \mathbf{L} + \sum_{\beta\gamma} j_{\alpha,\beta\gamma}^{\text{OAP}} \{L_\beta, L_\gamma\}, \quad (2)$$

where the first and second terms represent the OAM and OAP currents, respectively. After some algebra, we obtain

$$\mathbf{j}_\alpha^{\text{OAM}} = \frac{1}{4\pi} \text{Re} \left[\left(\frac{G_\alpha^{1,0} + G_\alpha^{0,-1}}{2} \right) \left(\mathbf{M} \times \frac{d\mathbf{M}}{dt} - i \frac{d\mathbf{M}}{dt} \right) \right], \quad (3)$$

$$j_{\alpha,\beta\gamma}^{\text{OAP}} = \frac{1}{8\pi} \text{Re} \left[\left(\frac{G_\alpha^{1,0} - G_\alpha^{0,-1}}{2} \right) \times \left(M_\beta \left(\mathbf{M} \times \frac{d\mathbf{M}}{dt} \right)_\gamma - i M_\beta \frac{dM_\gamma}{dt} + (\beta \leftrightarrow \gamma) \right) \right], \quad (4)$$

$$G_\alpha^{\mu,\nu} = \frac{J_{\text{ex}} \hbar^2}{m_e} \int dr' [g_\mu^R(r, r') \overset{\leftrightarrow}{\partial}_\alpha g_\nu^A(r', r)], \quad (5)$$

where $g^{R/A}$ represents retarded/advanced Green's function of the NM1/NM2/NM1 heterostructure, $\overset{\leftrightarrow}{\partial}_\alpha$ is the antisymmetric differential operator, and $\int dr'$ denotes the volume integral.

The OAM pumping current [Eq. (3)] has the same form as the spin pumping current [29], except for replacing the spin mixing conductance with the orbital mixing conductance [Eq. (5)]. The spin (orbital) mixing conductance arises from the scattering caused by an abrupt change of the spin (orbital) environment at an interface. Since the orbital space encompasses additional degrees of freedom (OAP), the orbital mixing conductance has more components than the spin mixing conductance. More specifically, 9 conductances are required to completely describe p -orbital scattering whereas 4 conductances (G^\uparrow , G^\downarrow , $\text{Re}[G^{\text{mix}}]$, $\text{Im}[G^{\text{mix}}]$) are sufficient for a full description of spin scattering [41]. The OAP pumping current derived in Eq. (4) corresponds to the additional components and is of the distinct form (including higher order terms in \mathbf{M}) from the OAM pumping current (thus from the spin pumping current as well). This OAP current corresponds to a flow of real-orbital-polarized electrons with zero OAM and lacks a counterpart in spin pumping, marking a qualitative distinction between orbital pumping and spin pumping.

As an example, when $\mathbf{M}(t)$ rotates in the zx plane ($\mathbf{M}(t) = \hat{\mathbf{z}} \cos \omega t + \hat{\mathbf{x}} \sin \omega t$), $j_z^{\text{OAM}} = \mathbf{j}_\alpha^{\text{OAM}} \cdot \mathbf{L}$ and $j_z^{\text{OAP}} = \sum_{\beta\gamma} j_{\alpha,\beta\gamma}^{\text{OAP}} \{L_\beta, L_\gamma\}$ become

$$j_z^{\text{OAM}} = \frac{\omega}{4\pi} \left\{ \text{Re}[G_L^+] L_y + \text{Im}[G_L^+] (L_x \cos \omega t - L_z \sin \omega t) \right\}, \quad (6)$$

$$j_z^{\text{OAP}} = \frac{\omega}{4\pi} \text{Im}[G_L^-] \left\{ (L_z, L_x) \cos 2\omega t - (L_z^2 - L_x^2) \sin 2\omega t \right\} + \frac{\omega}{4\pi} \text{Re}[G_L^-] \left\{ (L_y, L_z) \cos \omega t + (L_x, L_y) \sin \omega t \right\}, \quad (7)$$

where $G_L^\pm = (G_z^{1,0} \pm G_z^{0,-1})/2$. Here, j_z^{OAM} and j_z^{OAP} are the operator expressions of the OAM and OAP currents, respectively, which we use to show the dynamics of each orbital degree of freedom explicitly. Equations (6) and (7) predict that orbital pumping currents in ideal situations (i.e., no crystal field splitting) consist of a DC component carrying L_y , first-harmonic (1ω) ones carrying $L_x, L_z, \{L_y, L_z\}$, and $\{L_x, L_y\}$, and second-harmonic (2ω) ones carrying $\{L_z, L_x\}$ and $(L_z^2 - L_x^2)$.

Next, we examine orbital pumping in a more realistic situation, where the degeneracy of orbitals is lifted by crystal fields. We adopt a $sp3$ tight-binding model in a simple cubic lattice. With sp hybridization, the orbital nature of eigenstates varies with the crystal momentum. Such variation (called orbital texture) is common in real materials [12, 42].

We consider the same $\mathbf{M}(t)$ oscillation as above and calculate numerically the pumped orbital current using the linear response theory in the adiabatic limit (see Supplementary Materials (SM) for details [43]). We find that all of the orbital currents predicted by Eqs. (6) and (7) are pumped by the $\mathbf{M}(t)$ oscillation, although additional types of orbital currents are also pumped. Figure 2 presents some of the numerical results: DC OAM current ($j_z^{L_y, \text{DC}}$), DC OAP current ($j_z^{\{L_z, L_x\}, \text{DC}}$) [Fig. 2(a)],

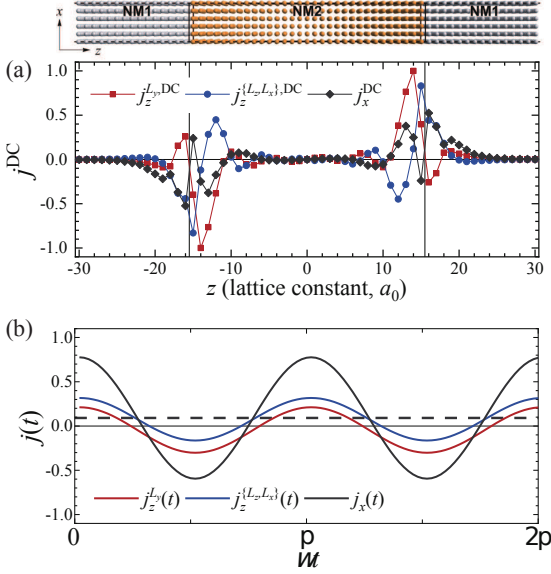


FIG. 2. (a) Spatial profile of DC pumping currents, $j_z^{L_y,DC}$ (red), $j_z^{L_z, L_x, DC}$ (blue), and j_x^{DC} (gray), driven by the time-dependent magnetic field, $\mathbf{L} \cdot \mathbf{M}(t)$ for $\mathbf{M}(t) = \hat{\mathbf{z}} \cos \omega t + \hat{\mathbf{x}} \sin \omega t$, on NM2 layer. (b) Temporal dependence of pumping currents $j(t)$ at the right interface ($z = 16 a_0$). The thick dashed horizontal line in (b) shows the DC component of transverse charge current $j_x(t)$.

and second-harmonic OAM current ($j_z^{L_y}(t)$), second-harmonic OAP current ($j_z^{L_z, L_x}(t)$) [Fig. 2(b)]. We note that the DC OAP current and the second-harmonic OAM current are unexpected from the analytic theory [Eqs. (6) and (7)]. We attribute these unexpected orbital currents to the fact that the crystal field splitting can convert OAM current to OAP current, and vice versa [26]. Note that the relatively short decay length of orbital currents in NM1 [Fig. 2(a)] arises from the orbital characters of the band structure used in our model. It increases with decreasing the orbital splitting [44], as demonstrated in SM [43].

The pumped OAM and OAP currents are converted to transverse charge currents j_x through the inverse orbital Hall effect [26, 45, 46] and inverse orbital-torsion Hall effect [26], respectively [Figs. 2(a) and (b)]. A recent orbital pumping experiment [39] reported a DC charge current and attributed it entirely to conversion from pumped DC OAM current [44]. However, the measured DC charge current may contain an additional contribution due to conversion from pumped DC OAP current. The converted charge current also contains a second-harmonic component since pumped OAM and OAP currents contain second-harmonic components [Fig. 2(b)]. The second-harmonic charge current remains unexplored experimentally. It is worth noting that the generalized pumping equation derived in SM [43] indicates that a d -orbital system may also produce a fourth-harmonic component. As a spin pumping current contains only DC and first-harmonic components [29], higher-harmonics pumping signals are a unique feature of orbital pumping.

In addition to orbital pumping, we find that the pumped

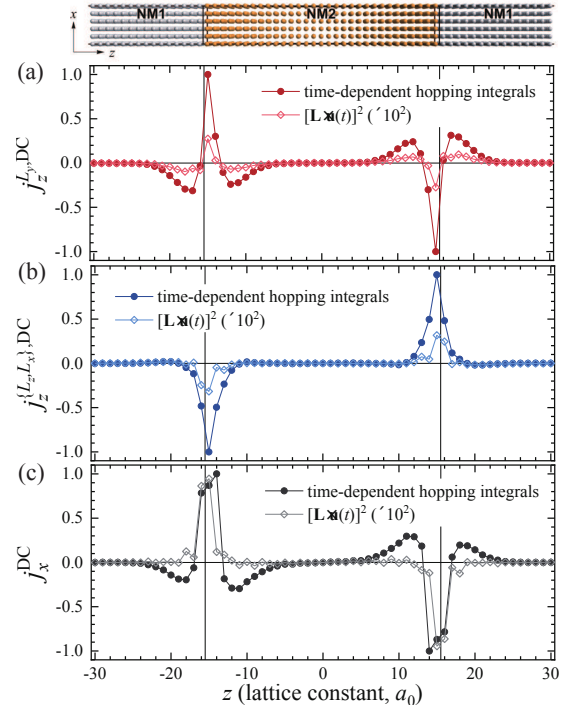


FIG. 3. Spatial profile of DC pumping currents (a) $j_z^{L_y,DC}$, (b) $j_z^{L_z, L_x, DC}$, and (c) j_x^{DC} driven by the lattice dynamics, which is imposed by time-dependent variations of tight-binding hopping integrals (solid circles) and $[\mathbf{L} \cdot \mathbf{u}(t)]^2$ for $\mathbf{u}(t) = \hat{\mathbf{z}} \cos \omega t + \hat{\mathbf{x}} \sin \omega t$ (open diamonds).

orbital current is converted to another orbital current, i.e., the orbital swapping effect. Analogous to the spin swapping effect [47–49], it results in the type I conversion (e.g., $j_z^{L_y,DC} \rightarrow j_z^{L_z, DC}$) and the type II conversion (e.g., $j_z^{L_z, DC} \rightarrow j_x^{DC}$), which can be called the OAM swapping effect and is in line with a recent theory [50]. We find that the OAP swapping effect also arises (see SM [43]). Similar to the orbital Hall effect [7], the orbital swapping effect arises even without SOC. But it vanishes in the absence of the orbital texture.

Orbital pumping by lattice dynamics–. In the second case, we explore orbital pumping due to lattice dynamics, which can be realized by a time-dependent variation of strain, i.e., a time-dependent deformation of crystal. For a crystal under arbitrary deformations, three effects need to be considered: variations of i) orbital splitting, ii) bonding lengths, and iii) bonding angles. Each factor manifests in the tight-binding model as corrections to on-site energies, magnitudes of hopping integrals, and directional cosines, respectively. By assuming the time-dependent hopping integrals to follow a power law of bonding length [51, 52], we integrate the periodic lattice dynamics driven by biaxial strains into our model and numerically calculate orbital pumping due to this lattice dynamics (see SM [43] for details).

We consider two biaxial strains in the zx plane with a phase difference, which makes the cubic lattice undergo a circularly rotating strain. It resembles a generation of phonon angu-

lar momentum (PAM) polarized along the y direction under surface acoustic wave [53]. Numerical calculations with the time-dependent hopping integrals show that DC OAM current [$j_z^{L_y,DC}$; Fig. 3(a)], DC OAP current [$j_z^{L_x,DC}$; Fig. 3(b)], and associated DC transverse charge current [j_z^{DC} ; Fig. 3(c)] are pumped. OAM pumping induced by lattice dynamics is the reverse process of crystal field torque [54], where non-equilibrium OAM, generated by external perturbations such as an electric field, is absorbed by the lattice. The reverse process of the OAP current may offer another mechanism of the crystal field torque, which has not been identified yet.

Orbital pumping driven by lattice dynamics can be understood through an OAP-type perturbation, which is qualitatively distinct from the previously considered perturbation, $\mathbf{L} \cdot \mathbf{M}(t)$, for the case of oscillating $\mathbf{M}(t)$. To demonstrate this, we consider the long-wavelength limit ($k \rightarrow 0$) of lattice vibration, where we may neglect the effects of spatial variations and focus on the time-dependent variations of orbital splitting (i.e., time-dependent lifting of orbital degeneracy in the analytic model). If the crystal experiences a strain along the \mathbf{u} direction, the energy of the p_u orbital becomes different from that of the other p orbitals perpendicular to it. It is important to note that the eigenvalue of $(\mathbf{L} \cdot \mathbf{u})^2$ with respect to the former is 0 while those with respect to the latter are 1. Therefore, the time-dependent strain in a p -orbital system can be modeled by a perturbation of $[\mathbf{L} \cdot \mathbf{u}(t)]^2$. In a general sense, a lattice distortion is time-reversal even, and thus the corresponding perturbation Hamiltonian should be expressed in terms of even-order products of the OAM operators, which is essentially OAP. The open diamonds in Fig. 3 confirm that the $[\mathbf{L} \cdot \mathbf{u}(t)]^2$ perturbation incorporated to the numerical model can reproduce the characteristics of orbital pumping from the lattice dynamics described by time-dependent hopping integrals in reasonable consistency, despite the simplicity of the model.

Further insight can be gained through a simplified analytic treatment. Assuming that all equilibrium orbitals are degenerate at the Γ point for simplicity, the Green's function for the perturbation of $[\mathbf{L} \cdot \mathbf{u}(t)]^2$ can be expressed as $g = g_0 I + (g_1 - g_0)[\mathbf{L} \cdot \mathbf{u}(t)]^2$. Utilizing Eqs. (3) and (4), we derive

$$\mathbf{j}_\alpha^{\text{OAM}} = \frac{1}{4\pi} \text{Re}[G_\alpha^{1,0}] \mathbf{u} \times \frac{d\mathbf{u}}{dt}, \quad (8)$$

$$j_{\alpha,\beta\gamma}^{\text{OAP}} = \frac{1}{8\pi} \text{Im}[G_\alpha^{1,0}] \frac{d(u_\beta u_\gamma)}{dt}, \quad (9)$$

which explain that both OAM and OAP currents are pumped by lattice dynamics. Equation (8) indicates the presence of nonzero DC OAM pumping when \mathbf{u} rotates in time, for example, $\mathbf{u}(t) = \hat{\mathbf{z}} \cos \omega t + \hat{\mathbf{x}} \sin \omega t$. OAM pumping induced by the rotating strain can be understood as the transfer of PAM to electron OAM [55]. Conversely, Eq. (9) suggests the absence of DC OAP pumping for a periodic \mathbf{u} , as demonstrated by its time average $(1/T) \int_0^T j_{\alpha,\beta\gamma}^{\text{OAP}} dt = (1/8\pi T) \text{Im}[G_\alpha^{1,0}] u_\beta(T) u_\gamma(T) \rightarrow 0$ as T increases. The emergence of DC OAP pumping in numerical calculations (Fig. 3) is attributed to the orbital texture, resulting in an interconversion between OAM and OAP,

as generally proven in Ref. [26]. Its detailed analytical description would require going beyond our simplified approach and considering the Green's function more complicated than $g = g_0 I + (g_1 - g_0)[\mathbf{L} \cdot \mathbf{u}(t)]^2$, which we leave for future work.

Discussion and outlook.— We demonstrated orbital pumping driven by either oscillating $\mathbf{M}(t)$ or lattice dynamics. In both pumping methods, not only OAM currents but also OAP currents are pumped. The simultaneous emergence of OAM and OAP pumping highlights the necessity of considering both orbital degrees of freedom when describing orbital dynamics. This is a fundamental requirement since a complete description of entire orbital degrees of freedom can be achieved only by incorporating both OAM and OAP operators. As a result, OAP pumping always plays a role in physical phenomena arising from OAM pumping. An important consequence is that OAP current contributes to orbital torque. It has been believed that orbital torque originates solely from the injection of OAM current [19]. However, the emergence of OAP current through magnetization dynamics suggests the existence of its inverse process: the generation of magnetic torque through the injection of OAP current. This previously unrecognized inverse process, which we term "OAP torque", introduces a new dimension to the understanding of orbital torque. Moreover, the Onsager reciprocity between orbital pumping and orbital torque is validated only when one considers both OAM and OAP contributions.

Our theory of orbital pumping offers an exploitable method for generating and detecting the OAP degree of freedom. We note that previous suggestions in Ref. [26] rely on twisted heterostructures, which can be challenging to implement, or on low-gap semiconductors with limited availability of the required materials. In contrast, the high-harmonics pumping, driven by the OAP degree of freedom, can be realized with various materials. We also note that this property stems from the distinct behaviors of high-order products of L operators with respect to rotational transformations. Thus, it is a general property that is not limited to p -orbital systems.

Furthermore, orbital pumping is not limited to multilayer structures. Recalling that the spin motive force is a continuum version of spin pumping [56], we anticipate the presence of an orbital motive force when a single-layer system exhibits an inhomogeneous crystal field. Thus, the orbital motive force would encompass OAP contributions, which lack their spin counterparts. Notably, the physical properties of the orbital motive force would differ from those of the spin motive force due to the presence of orbital texture, a factor not accounted for in the theory of the spin motive force. The exploration of this topic remains a subject for future work.

Lastly, our work sheds light on the transfer of angular momentum between electrons and phonons. Theoretical estimations [57–59] and experimental measurements [53, 60, 61] illustrate that PAM can have a considerable magnitude contrary to early assumptions and plays a nontrivial role in various phenomena such as magnetization relaxation [62] and ultrafast demagnetization [63, 64]. Intriguingly, recent many-body treatment [65] shows that a complete picture of angular momen-

tum transfer between electron and phonon subsystems requires OAM as a key ingredient since the electron-phonon coupling is independent of spin. The strain-induced orbital pumping weighs heavily on this connection of orbital and lattice and call for a wider viewpoint on PAM dynamics [55, 66, 67] assisted by the orbital degree of freedom [68].

Note added.— During the preparation of our manuscript, we became aware of a recent theoretical work on orbital pumping that focuses only on OAM pumping induced by magnetization dynamics [40].

This work was supported by the National Research Foundation of Korea (NRF) funded by the Ministry of Science and ICT (2020R1A2C3013302, 2022M3I7A2079267) and the KIST Institutional Program. S.H. and H.-W.L. were supported by the Samsung Science and Technology Foundation (BA-1501-51).

**S.H. and H.-W.K. contributed equally to this work.

* hwl@postech.ac.kr

† kjlee@kaist.ac.kr

‡ kwk@kist.re.kr

- [1] D. Go, D. Jo, H.-W. Lee, M. Kläui, and Y. Mokrousov, *Orbitronics: Orbital currents in solids*, *Europhys. Lett.* **135**, 37001 (2021).
- [2] B. A. Bernevig, T. L. Hughes, and S.-C. Zhang, *Orbitronics: The Intrinsic Orbital Current in p -Doped Silicon*, *Phys. Rev. Lett.* **95**, 066601 (2005).
- [3] T. Tanaka, H. Kontani, M. Naito, T. Naito, D. S. Hirashima, K. Yamada, and J. Inoue, *Intrinsic spin Hall effect and orbital Hall effect in $4d$ and $5d$ transition metals*, *Phys. Rev. B* **77**, 165117 (2008).
- [4] H. Kontani, T. Tanaka, D. S. Hirashima, K. Yamada, and J. Inoue, *Giant Intrinsic Spin and Orbital Hall Effects in Sr_2MO_4 ($M = \text{Ru, Rh, Mo}$)*, *Phys. Rev. Lett.* **100**, 096601 (2008).
- [5] H. Kontani, T. Tanaka, D. S. Hirashima, K. Yamada, and J. Inoue, *Giant Orbital Hall Effect in Transition Metals: Origin of Large Spin and Anomalous Hall Effects*, *Phys. Rev. Lett.* **102**, 016601 (2009).
- [6] I. V. Tokatly, *Orbital momentum Hall effect in p -doped graphene*, *Phys. Rev. B* **82**, 161404(R) (2010).
- [7] D. Go, D. Jo, C. Kim, and H.-W. Lee, *Intrinsic Spin and Orbital Hall Effects from Orbital Texture*, *Phys. Rev. Lett.* **121**, 086602 (2018).
- [8] D. Jo, D. Go, and H.-W. Lee, *Gigantic intrinsic orbital Hall effects in weakly spin-orbit coupled metals*, *Phys. Rev. B* **98**, 214405 (2018).
- [9] S. Bhowal and G. Vignale, *Orbital Hall effect as an alternative to valley Hall effect in gapped graphene*, *Phys. Rev. B* **103**, 195309 (2021).
- [10] T. P. Cysne, M. Costa, L. M. Canonico, M. B. Nardelli, R. Muniz, and T. G. Rappoport, *Disentangling Orbital and Valley Hall Effects in Bilayers of Transition Metal Dichalcogenides*, *Phys. Rev. Lett.* **126**, 056601 (2021).
- [11] Y.-G. Choi, D. Jo, K.-H. Ko, D. Go, K.-H. Kim, H. G. Park, C. Kim, B.-C. Min, G.-M. Choi, and H.-W. Lee, *Observation of the orbital Hall effect in a light metal Ti*, *Nature* **619**, 52 (2023).
- [12] H.-W. Ko, H.-J. Park, G. Go, J. H. Oh, K.-W. Kim, and K.-J. Lee, *Role of orbital hybridization in anisotropic magnetoresistance*, *Phys. Rev. B* **101**, 184413 (2020).
- [13] S. Ding, Z. Liang, D. Go, C. Yun, M. Xue, Z. Liu, S. Becker, W. Yang, H. Du, C. Wang, Y. Yang, G. Jakob, M. Kläui, Y. Mokrousov, and J. Yang, *Observation of the Orbital Rashba-Edelstein Magnetoresistance*, *Phys. Rev. Lett.* **128**, 067201 (2022).
- [14] J. Sinova, D. Culcer, Q. Niu, N. Sinitsyn, T. Jungwirth, and A. H. MacDonald, *Universal Intrinsic Spin Hall Effect*, *Phys. Rev. Lett.* **92**, 126603 (2004).
- [15] J. Sinova, S. O. Valenzuela, J. Wunderlich, C. H. Back, and T. Jungwirth, *Spin Hall effects*, *Rev. Mod. Phys.* **87**, 1213 (2015).
- [16] H. Nakayama, Y. Kanno, H. An, T. Tashiro, S. Haku, A. Nomura, and K. Ando, *Rashba-Edelstein Magnetoresistance in Metallic Heterostructures*, *Phys. Rev. Lett.* **117**, 116602 (2016).
- [17] J. C. Slonczewski, *Current-driven excitation of magnetic multilayers*, *J. Magn. Magn. Mater.* **159**, L1 (1996).
- [18] L. Berger, *Emission of spin waves by a magnetic multilayer traversed by a current*, *Phys. Rev. B* **54**, 9353 (1996).
- [19] D. Go and H.-W. Lee, *Orbital torque: Torque generation by orbital current injection*, *Phys. Rev. Res.* **2**, 013177 (2020).
- [20] Z. C. Zheng, Q. X. Guo, D. Jo, D. Go, L. H. Wang, H. C. Chen, W. Yin, X. M. Wang, G. H. Yu, W. He, H.-W. Lee, J. Teng, and T. Zhu, *Magnetization switching driven by current-induced torque from weakly spin-orbit coupled Zr*, *Phys. Rev. Res.* **2**, 013127 (2020).
- [21] Y. Tazaki, Y. Kageyama, H. Hayashi, T. Harumoto, T. Gao, J. Shi, and K. Ando, *Current-induced torque originating from orbital current*, arXiv:2004.09165.
- [22] D. Lee, D. Go, H.-J. Park, W. Jeong, H.-W. Ko, D. Yun, D. Jo, S. Lee, G. Go, J. H. Oh, K.-J. Kim, B.-G. Park, B.-C. Min, H. C. Koo, H.-W. Lee, O. Lee, and K.-J. Lee, *Orbital torque in magnetic bilayers*, *Nat. Commun.* **12**, 6710 (2021).
- [23] J. Kim, D. Go, H. Tsai, D. Jo, K. Kondou, H.-W. Lee, and Y. Otani, *Nontrivial torque generation by orbital angular momentum injection in ferromagnetic-metal/Cu/ Al_2O_3 trilayers*, *Phys. Rev. B* **103**, L020407 (2021).
- [24] G. Sala and P. Gambardella, *Giant orbital Hall effect and orbital-to-spin conversion in $3d$, $5d$, and $4f$ metallic heterostructures*, *Phys. Rev. Res.* **4**, 033037 (2022).
- [25] L. Salemi and P. M. Oppeneer, *First-principles theory of intrinsic spin and orbital Hall and Nernst effects in metallic monoatomic crystals*, *Phys. Rev. Mater.* **6**, 095001 (2022).
- [26] S. Han, H.-W. Lee, and K.-W. Kim, *Orbital Dynamics in Centrosymmetric Systems*, *Phys. Rev. Lett.* **128**, 176601 (2022).
- [27] D. J. Thouless, *Quantization of particle transport*, *Phys. Rev. B* **27**, 6083 (1983).
- [28] R. Citro and M. Aidelsburger, *Thouless pumping and topology*, *Nat. Rev. Phys.* **5**, 87 (2023).
- [29] Y. Tserkovnyak, A. Brataas, and G. E. W. Bauer, *Enhanced Gilbert Damping in Thin Ferromagnetic Films*, *Phys. Rev. Lett.* **88**, 117601 (2002).
- [30] K.-W. Kim, J.-H. Moon, K.-J. Lee, and H.-W. Lee, *Prediction of Giant Spin Motive Force due to Rashba Spin-Orbit Coupling*, *Phys. Rev. Lett.* **108**, 217202 (2012).
- [31] G. Tatara, N. Nakabayashi, and K.-J. Lee, *Spin motive force induced by Rashba interaction in the strong sd coupling regime*, *Phys. Rev. B* **87**, 054403 (2013).
- [32] W. M. Saslow, *Spin pumping of current in non-uniform conducting magnets*, *Phys. Rev. B* **76**, 184434 (2007).
- [33] R. Cheng, J. Xiao, Q. Niu, and A. Brataas, *Spin Pumping and Spin-Transfer Torques in Antiferromagnets*, *Phys. Rev. Lett.* **113**, 057601 (2014).
- [34] K. Chen and S. Zhang, *Spin Pumping in the Presence of Spin-Orbit Coupling*, *Phys. Rev. Lett.* **114**, 126602 (2015).

- [35] O. Mosendz, J. E. Pearson, F. Y. Fradin, G. E. W. Bauer, S. D. Bader, and A. Hoffmann, Quantifying Spin Hall Angles from Spin Pumping: Experiments and Theory, *Phys. Rev. Lett.* **104**, 046601 (2010).
- [36] K. Ando, S. Takahashi, J. Ieda, Y. Kajiwara, H. Nakayama, T. Yoshino, K. Harii, Y. Fujikawa, M. Matsuo, S. Maekawa, and E. Saitoh, Inverse spin-Hall effect induced by spin pumping in metallic system. *J. Appl. Phys.* **109**, 103913 (2011).
- [37] Y. Tserkovnyak, A. Brataas, G. E. W. Bauer, and B. I. Halperin, Nonlocal magnetization dynamics in ferromagnetic heterostructures, *Rev. Mod. Phys.* **77**, 1375 (2005).
- [38] E. Santos, J.E. Abrão, D. Go, L.K. de Assis, Y. Mokrousov, J.B.S. Mendes, and A. Azevedo, Inverse Orbital Torque via Spin-Orbital Intertwined States, *Phys. Rev. Appl.* **19**, 014069 (2023).
- [39] H. Hayashi and K. Ando, Observation of orbital pumping, arXiv:2304.05266 (2023).
- [40] D. Go, K. Ando, A. Pezo, S. Blügel, A. Manchon, and Y. Mokrousov, Orbital Pumping by Magnetization Dynamics in Ferromagnets, arXiv:2309.14817 (2023).
- [41] A. Brataas, Y. V. Nazarov, and G. E. W. Bauer, Finite-Element Theory of Transport in Ferromagnet–Normal Metal Systems, *Phys. Rev. Lett.* **84**, 2481 (2000).
- [42] S. Han, H.-W. Lee, and K.-W. Kim, Microscopic study of orbital textures, *Curr. Appl. Phys.* **50**, 13 (2023).
- [43] See Supplemental Materials for details.
- [44] D. Go, D. Jo, K.-W. Kim, S. Lee, M.-G. Kang, B.-G. Park, S. Blügel, H.-W. Lee, and Y. Mokrousov, Long-Range Orbital Torque by Momentum-Space Hotspots, *Phys. Rev. Lett.* **130**, 246701 (2023).
- [45] P. Wang, Z. Feng, Y. Yang, D. Zhang, Q. Liu, Z. Xu, Z. Jia, Y. Wu, G. Yu, X. Xu, and Y. Jiang, Inverse orbital Hall effect and orbitronic terahertz emission observed in the materials with weak spin-orbit coupling, *npj Quantum Mater.* **8**, 28 (2023).
- [46] Y. Xu, F. Zhang, A. Fert, H.-Y. Jaffres, Y. Liu, R. Xu, Y. Jiang, H. Cheng, and W. Zhao, Orbitronics: Light-induced Orbit Currents in Terahertz Emission Experiments, arXiv:2307.03490 (2023).
- [47] M. B. Lifshits and M. I. Dyakonov, Swapping Spin Currents: Interchanging Spin and Flow Directions, *Phys. Rev. Lett.* **103**, 186601 (2009).
- [48] S. Sadjina, A. Brataas, and A. G. Mal'shukov, Intrinsic spin swapping, *Phys. Rev. B* **85**, 115306 (2012).
- [49] H. B. M. Saidaoui and A. Manchon, Spin-Swapping Transport and Torques in Ultrathin Magnetic Bilayers, *Phys. Rev. Lett.* **117**, 036601 (2016).
- [50] A. Manchon, A. Pezo, K.-W. Kim, and K.-J. Lee, Orbital diffusion, polarization and swapping in centrosymmetric metals, arXiv:2310.04763 (2023).
- [51] S. Froyen and W. A. Harrison, Elementary prediction of linear combination of atomic orbitals matrix elements, *Phys. Rev. B* **20**, 2420 (1979).
- [52] W. A. Harrison, *Electronic Structure and the Properties of Solids* (Freeman, San Francisco, 1980).
- [53] R. Sasaki, Y. Nii, and Y. Onose, Magnetization control by angular momentum transfer from surface acoustic wave to ferromagnetic spin moments, *Nat. Commun.* **12**, 2599 (2021).
- [54] D. Go, F. Freimuth, J.-P. Hanke, F. Xue, O. Gomonay, K.-J. Lee, S. Blügel, P. M. Haney, H.-W. Lee, and Y. Mokrousov, Theory of current-induced angular momentum transfer dynamics in spin-orbit coupled systems, *Phys. Rev. Res.* **2**, 033401 (2020).
- [55] D. Yao and S. Murakami, Chiral-phonon-induced current in helical crystals, *Phys. Rev. B* **105**, 184412 (2022).
- [56] S. Zhang and S. S.-L. Zhang, Generalization of the Landau-Lifshitz-Gilbert Equation for Conducting Ferromagnets, *Phys. Rev. Lett.* **102**, 086601 (2009).
- [57] L. Zhang and Q. Niu, Angular Momentum of Phonons and the Einstein-de Haas Effect, *Phys. Rev. Lett.* **112**, 085503 (2014).
- [58] L. Zhang and Q. Niu, Chiral Phonons at High-Symmetry Points in Monolayer Hexagonal Lattices, *Phys. Rev. Lett.* **115**, 115502 (2015).
- [59] Y. Ren, C. Xiao, D. Saparov, and Q. Niu, Phonon Magnetic Moment from Electronic Topological Magnetization, *Phys. Rev. Lett.* **127**, 186403 (2021).
- [60] H. Zhu, J. Yi, M.-Y. Li, J. Xiao, L. Zhang, C.-W. Yang, R. A. Kaindl, L.-J. Li, Y. Wang, and X. Zhang, Observation of chiral phonons, *Science* **359**, 579 (2018).
- [61] J. Holanda, D. S. Maior, A. Azevedo, and S. M. Rezende, Detecting the phonon spin in magnon-phonon conversion experiments, *Nat. Phys.* **14**, 500 (2018).
- [62] S. Streib, H. Keshtgar, and G. E. W. Bauer, Damping of Magnetization Dynamics by Phonon Pumping, *Phys. Rev. Lett.* **121**, 027202 (2018).
- [63] C. Dornes, Y. Acremann, M. Savoini, M. Kubli, M. J. Neugebauer, E. Abreu, L. Huber, G. Lantz, C. A. F. Vaz, H. Lemke, E. M. Bothschafter, M. Porer, V. Esposito, L. Rettig, M. Buzzi, A. Alberca, Y. W. Windsor, P. Beaud, U. Staub, D. Zhu, S. Song, J. M. Glownia, and S. L. Johnson, The ultrafast Einstein–de Haas effect, *Nature* **565**, 209 (2019).
- [64] S. R. Tauchert, M. Volkov, D. Ehberger, D. Kazenwadel, M. Evers, H. Lange, A. Donges, A. Book, W. Kreuzpaintner, U. Nowak, and P. Baum, Polarized phonons carry angular momentum in ultrafast demagnetization, *Nature* **602**, 73 (2022).
- [65] J. H. Mentink, M. I. Katsnelson, and M. Lemoshko, Quantum many-body dynamics of the Einstein–de Haas effect, *Phys. Rev. B* **99**, 064428 (2019).
- [66] M. Hamada and S. Murakami, Conversion between electron spin and microscopic atomic rotation, *Phys. Rev. Res.* **2**, 023275 (2020).
- [67] D. Yao and S. Murakami, Conversion of phonon angular momentum into magnons in ferromagnets, arXiv:2304.14000 (2023).
- [68] C. Xiao, Y. Ren, and B. Xiong, Adiabatically induced orbital magnetization, *Phys. Rev. B* **103**, 115432 (2021).

Supplemental Material for "Theory of Orbital Pumping"

I. GENERAL PUMPING FORMULA FOR ARBITRARY ORBITAL SYSTEMS

A. Generalized algebra for high- l orbital spaces

In the case of spin, one can completely describe the dynamics using the Pauli matrix, enabling us to represent arbitrary traceless operators as vectors. Consequently, the pumping formula can also be expressed in vector form. However, in the case of orbitals with angular momentum quantum number l , it is imperative to define a vector space of $(2l+1)^2$ dimensions, leading to the necessity of generalizing the dot product and cross product. This section will provide these definitions and outline their essential algebraic properties. In the following section, we will employ these concepts to demonstrate the straightforward generalization of the pumping formula.

We define a new symbol " \doteq " to denote the mapping of an $(2l+1) \times (2l+1)$ matrix A to an $(2l+1)^2$ -dimensional vector as follows,

$$\mathbf{A} \doteq A, \quad (\text{S1})$$

where $A = A_i L_i$ (Einstein convention), $\text{Tr}[L_i L_j] = 2\delta_{ij}$, and $A_i = \text{Tr}[A L_i]/2$. The orthogonality guarantees the uniqueness and existence of the representation. We can generalize the cross product and dot product that map $\mathbb{R}^{n^2} \times \mathbb{R}^{n^2}$ to \mathbb{R}^{n^2} as,

$$\mathbf{A} \odot \mathbf{B} \doteq \frac{1}{2}\{A, B\}, \quad (\text{S2})$$

$$\mathbf{A} \otimes \mathbf{B} \doteq \frac{1}{2i}[A, B]. \quad (\text{S3})$$

Below, we present some useful properties of generalized dot and cross products.

1. Property 1: Bilinearity

$$(\mathbf{A} + \mathbf{B}) \odot (\mathbf{C} + \mathbf{D}) = \mathbf{A} \odot \mathbf{B} + \mathbf{B} \odot \mathbf{C} + \mathbf{A} \odot \mathbf{D} + \mathbf{B} \odot \mathbf{D}, \quad (\text{S4})$$

$$(\mathbf{A} + \mathbf{B}) \otimes (\mathbf{C} + \mathbf{D}) = \mathbf{A} \otimes \mathbf{B} + \mathbf{B} \otimes \mathbf{C} + \mathbf{A} \otimes \mathbf{D} + \mathbf{B} \otimes \mathbf{D}. \quad (\text{S5})$$

2. Property 2: (anti)commutativity

$$\mathbf{A} \otimes \mathbf{B} = -\mathbf{B} \otimes \mathbf{A}, \quad (\text{S6})$$

$$\mathbf{A} \odot \mathbf{B} = \mathbf{B} \odot \mathbf{A}. \quad (\text{S7})$$

3. Property 3: Representation of matrix multiplication

$$\mathbf{AB} = \mathbf{A} \odot \mathbf{B} + i\mathbf{A} \otimes \mathbf{B}. \quad (\text{S8})$$

c.f. $(\mathbf{a} \cdot \boldsymbol{\sigma})(\mathbf{b} \cdot \boldsymbol{\sigma}) = \mathbf{a} \cdot \mathbf{b} + i(\mathbf{a} \times \mathbf{b}) \cdot \boldsymbol{\sigma}$ for the spin case.

4. Property 4: Traces

Definition: $\text{Tr}_v[\mathbf{A}] \doteq \text{Tr}[A]$.

$$\text{Tr}_v[\mathbf{A} \otimes \mathbf{B}] = 0, \quad (\text{S9})$$

$$\text{Tr}_v[\mathbf{A} \odot \mathbf{B}] = 2\mathbf{A} \cdot \mathbf{B}. \quad (\text{S10})$$

5. *Property 5: Completeness relation.*

$$\text{Tr}_v[\mathbf{A} \odot \mathbf{B}] = \frac{1}{2} \text{Tr}_v[\mathbf{A} \odot L_i] \text{Tr}_v[L_i \odot \mathbf{B}]. \quad (\text{S11})$$

6. *Property 6: Trace of matrix multiplication.*

$$\text{Tr}[AB] = 2\mathbf{A} \cdot \mathbf{B}, \quad (\text{S12})$$

$$\text{Tr}[ABC] = 2\mathbf{A} \cdot (\mathbf{B} \odot \mathbf{C} + i\mathbf{B} \otimes \mathbf{C}), \quad (\text{S13})$$

where $\mathbf{A} \cdot \mathbf{B} = A_i B_i$.

7. *Property 7: Jacobi identities*

$$\mathbf{A} \otimes (\mathbf{B} \otimes \mathbf{C}) + \mathbf{B} \otimes (\mathbf{C} \otimes \mathbf{A}) + \mathbf{C} \otimes (\mathbf{A} \otimes \mathbf{B}) = 0, \quad (\text{S14})$$

$$\mathbf{A} \otimes (\mathbf{B} \odot \mathbf{C}) + \mathbf{B} \otimes (\mathbf{C} \odot \mathbf{A}) + \mathbf{C} \otimes (\mathbf{A} \odot \mathbf{B}) = 0. \quad (\text{S15})$$

8. *Property 8: Non-associativity relations*

$$\mathbf{A} \odot (\mathbf{B} \odot \mathbf{C}) - (\mathbf{A} \odot \mathbf{B}) \odot \mathbf{C} = -\mathbf{B} \otimes (\mathbf{C} \otimes \mathbf{A}), \quad (\text{S16})$$

$$\mathbf{A} \otimes (\mathbf{B} \otimes \mathbf{C}) - (\mathbf{A} \otimes \mathbf{B}) \otimes \mathbf{C} = -\mathbf{B} \otimes (\mathbf{C} \otimes \mathbf{A}), \quad (\text{S17})$$

$$\mathbf{A} \otimes (\mathbf{B} \odot \mathbf{C}) - (\mathbf{A} \otimes \mathbf{B}) \odot \mathbf{C} = -\mathbf{B} \odot (\mathbf{C} \otimes \mathbf{A}). \quad (\text{S18})$$

c.f. The second relation is equivalent to the first Jacobi identity.

9. *Property 9: Triple scalar products*

$$\mathbf{A} \cdot (\mathbf{B} \odot \mathbf{C}) = (\mathbf{A} \odot \mathbf{B}) \cdot \mathbf{C} \quad (= \frac{1}{4} \text{Tr}[ABC + ACB]), \quad (\text{S19})$$

$$\mathbf{A} \cdot (\mathbf{B} \otimes \mathbf{C}) = (\mathbf{A} \otimes \mathbf{B}) \cdot \mathbf{C} \quad (= \frac{1}{4i} \text{Tr}[ABC - ACB]). \quad (\text{S20})$$

c.f. $\mathbf{A} \cdot (\mathbf{B} \times \mathbf{C}) = (\mathbf{A} \times \mathbf{B}) \cdot \mathbf{C}$ for usual cross product.

10. *Property 10: spin limit*

For $L_i = \sigma_i$ ($i = 0, 1, 2, 3$),

$$\mathbf{A} \odot \mathbf{B} \doteq (\mathbf{A} \cdot \mathbf{B}, A_0 B_1 + B_0 A_1, A_0 B_2 + A_2 B_0, A_0 B_3 + A_3 B_0), \quad (\text{S21})$$

$$\mathbf{A} \otimes \mathbf{B} \doteq (0, A_2 B_3 - A_3 B_2, A_3 B_1 - A_1 B_3, A_1 B_2 - A_2 B_1). \quad (\text{S22})$$

11. Property 11: Equation of motion

For physical operator A and Hamiltonian H ,

$$\frac{dA}{dt} = \frac{1}{i\hbar}[H, A] \doteq \frac{2}{\hbar}\mathbf{H} \otimes \mathbf{A}. \quad (\text{S23})$$

B. The Green's function formalism for orbital pumping

In this section, we derive a pumping formula applicable to arbitrary orbital systems with angular momentum quantum number l . We extend the formula derived in the reference [1] for spin pumping, utilizing the Green's function approach, to operate even in states with higher angular momentum ($l \geq 1/2$). For state with total angular momentum l , we need $(2l + 1)^2$ -dimensional vector space to completely describe pumping effects. We define unit vector in $(2l + 1)^2$ space as follows,

$$\hat{\alpha} \doteq L_\alpha. \quad (\text{S24})$$

Then ν -direction total current is given by,

$$\mathbf{j}_\nu = \frac{\hbar}{4\pi} \frac{J_{ex}\hbar^2}{m_e i} \int dr' \left[\mathbf{g}^R(r, r') \hat{\alpha} \overleftrightarrow{\partial}_\nu \mathbf{g}^A(r', r) \right] \frac{du_\alpha}{dt}, \quad (\text{S25})$$

where $\mathbf{g}^{R/A}(r, r')$ is retarded and advanced Green's function defined in $(2l + 1)^2$ -dimensional vector space and $(du_\alpha/dt)\hat{\alpha}$ constitutes external perturbations also defined in $(2l + 1)^2$ -dimensional vector space. Then, we use orbital algebra introduced in the previous section to simplify above equation. Using generalized products defined in previous section, the orbital current is given by,

$$\mathbf{j}_\nu = \frac{\hbar}{4\pi} \frac{J_{ex}\hbar^2}{m_e} \text{Im} \int dr' \times \left[\left(\mathbf{g}^R(r, r') \circ \hat{\alpha} \right) \circ \overleftrightarrow{\partial}_\nu \mathbf{g}^A(r', r) - \left(\mathbf{g}^R(r, r') \otimes \hat{\alpha} \right) \otimes \overleftrightarrow{\partial}_\nu \mathbf{g}^A(r', r) + i \left(\mathbf{g}^R(r, r') \circ \hat{\alpha} \right) \otimes \overleftrightarrow{\partial}_\nu \mathbf{g}^A(r', r) + i \left(\mathbf{g}^R(r, r') \otimes \hat{\alpha} \right) \circ \overleftrightarrow{\partial}_\nu \mathbf{g}^A(r', r) \right] \frac{du_\alpha}{dt}. \quad (\text{S26})$$

By projecting the expression for $\mathbf{g}^{R/A}$ onto unit vectors, we can obtain pumping expressions with a generalized mixing conductance,

$$\mathbf{j}_\nu = \frac{\hbar}{4\pi} \frac{J_{ex}\hbar^2}{m_e} \int dr' \times \sum_{\beta\gamma} \text{Im} [g_\beta^R(r, r') \overleftrightarrow{\partial}_\nu g_\gamma^A(r', r)] [(\hat{\beta} \circ \hat{\alpha}) \circ \hat{\gamma} - (\hat{\beta} \otimes \hat{\alpha}) \otimes \hat{\gamma}] + \text{Re} [g_\beta^R(r, r') \overleftrightarrow{\partial}_\nu g_\gamma^A(r', r)] [(\hat{\beta} \circ \hat{\alpha}) \otimes \hat{\gamma} + (\hat{\beta} \otimes \hat{\alpha}) \circ \hat{\gamma}] \frac{du_\alpha}{dt}, \quad (\text{S27})$$

where $g_m^{R/A} = \mathbf{g}^{R/A} \cdot \hat{\mathbf{m}}$.

II. ORBITAL PUMPING BASED ON THE SCATTERING MATRIX APPROACH

In this subsection, we show that the pumped orbital current by the magnetization dynamics using the scattering matrix approach [2] is consistent with that of the Green's function approach. Following the conventional scattering matrix approach [2], the pumped current density operator j_α where α is the flow direction is given by,

$$j_\alpha / (-e) = \frac{\partial n_\alpha}{\partial X} \frac{dX(t)}{dt}, \quad (\text{S28})$$

$$\frac{\partial n_\alpha}{\partial X} = \frac{1}{4\pi i} \frac{\partial S}{\partial X} S^\dagger + \text{h.c.}, \quad (\text{S29})$$

where $X(t)$ is a time-dependent system parameter, $\partial n_\alpha / \partial X$ is 3×3 emissivity matrix along α direction, and S is the 3×3 scattering matrix in p -orbital space. We then define the orbital mixing conductance as the orbital counterpart of the spin mixing conductance,

$$G^{i,j} \doteq 1 - r_i r_j^*, \quad (\text{S30})$$

where r_i and r_j are the reflection coefficients. Now we calculate the pumped orbital currents by the magnetization dynamics where the Hamiltonian is given by,

$$H(t) = \mathbf{L} \cdot \mathbf{M}(t). \quad (\text{S31})$$

For this case, scattering matrix is given by,

$$S = \sum_m r_m |m\rangle\langle m|, \quad (\text{S32})$$

where $|m\rangle$ is the eigenstate of the Eq. (S31). Then, the pumped OAM and OAP currents are given by,

$$\mathbf{j}_\alpha^{\text{OAM}} = \frac{1}{8\pi} \text{Re} \left[\left(\frac{G^{1,0} + G^{0,-1}}{2} \right) \left(\mathbf{M} \times \frac{d\mathbf{M}}{dt} - i \frac{d\mathbf{M}}{dt} \right) \right], \quad (\text{S33})$$

$$j_{\alpha,\beta\gamma}^{\text{OAP}} = \frac{1}{16\pi} \text{Re} \left[\left(\frac{G^{1,0} - G^{0,-1}}{2} \right) \times \left(M_\beta \left(\mathbf{M} \times \frac{d\mathbf{M}}{dt} \right)_\gamma - i M_\beta \frac{dM_\gamma}{dt} + (\beta \leftrightarrow \gamma) \right) \right], \quad (\text{S34})$$

where α is the surface-normal direction. We can see there is direct mapping between pumped orbital currents calculated by Green's function approach. The same conclusion can be drawn for the orbital pumping by the lattice dynamics.

III. LINEAR RESPONSE CALCULATION

We consider currents carrying a physical quantity Q . An increase of Q in the region less than the $(\ell + 1)$ -th layer is given by,

$$\frac{dN^Q(\ell)}{dt} = \frac{d}{dt} \left\langle \sum_{i=-\infty}^{\ell} Q^{(i)}(t) \right\rangle, \quad Q^{(i)}(t) = \sum_{\alpha,\alpha'} C_{i\alpha}^\dagger(t) Q_{i\alpha,\alpha'} C_{i\alpha'}(t).$$

From the Heisenberg equation of motion, the increasing rate of Q is expressed as,

$$\frac{dN^Q(\ell)}{dt} = \frac{1}{i\hbar} \left\langle \left[\sum_{i=-\infty}^{\ell} Q^{(i)}(t), \sum C_{i_1\alpha_1}^\dagger H_{\alpha_1,\alpha_2}^{i_1,i_2} C_{i_2\alpha_2} \right] \right\rangle,$$

where H is the Hamiltonian matrix. Using the commutation relations of $\{C_{i\alpha}, C_{j\alpha'}^\dagger\} = \delta_{ij}\delta_{\alpha\alpha'}$, we derive an increase of Q in terms of the generation and transfer terms:

$$\frac{dN^Q(\ell)}{dt} = W_L^Q(\ell) + I_L^Q(\ell).$$

Here, $W_L^Q(\ell)$ is the generation rate and $I_L^Q(\ell)$ is the current of increasing Q in the region less than $(\ell + 1)$,

$$I_L^Q(\ell) = \frac{1}{i\hbar} Q_{\ell\alpha,\ell\alpha'} \left\langle C_{\ell\alpha}^\dagger H_{\alpha',\alpha_1}^{\ell,\ell+1} C_{\ell+1\alpha_1} - C_{\ell+1\alpha_1}^\dagger H_{\alpha_1,\alpha}^{\ell+1,\ell} C_{\ell\alpha'} \right\rangle.$$

By defining the lesser Green function by $\langle C_\alpha^\dagger C_\beta \rangle = -i\hbar G_{\beta\alpha}^<$, we arrive at

$$I_L^Q(\ell) = 2 \text{Re Tr} \left[H^{\ell+1,\ell} Q_{\ell,\ell} G^{<(\ell,\ell+1)} \right].$$

In a similar way, we can calculate an increase of Q in the region greater than the ℓ -th layer that is given by,

$$I_R^Q(\ell) = 2 \text{Re Tr} \left[H^{\ell,\ell+1} Q_{\ell+1,\ell+1} G^{<(\ell+1,\ell)} \right].$$

In an averaged sense, we define the current carrying Q as,

$$\begin{aligned} j^Q(\ell) &= \frac{1}{2} \left[I_R^Q(\ell - 1) - I_L^Q(\ell) \right] \\ &= \text{Re Tr} \left[Q_{\ell,\ell} \left(G^{<(\ell,\ell-1)} H^{\ell-1,\ell} - G^{<(\ell,\ell+1)} H^{\ell+1,\ell} \right) \right]. \end{aligned} \quad (\text{S35})$$

If a time-dependent term $U(t)$ in the Hamiltonian is slow enough relative to electron dynamics, we can treat its time-derivative $\dot{U}(t)$ as a perturbation. Then, the lesser Green function is expressed as

$$G^<(t, t) = -\frac{1}{2\pi\hbar} \int dE f_0(E) \left[G^C(E) + i\hbar \left(\frac{\partial G^R}{\partial E} \dot{U}(t) G^C(E) - G^C(E) \dot{U}(t) \frac{\partial G^A}{\partial E} \right) + \dots \right].$$

Here, $f_0(E)$ is the Fermi-Dirac distribution and $G^C(E) \equiv G^R(E) - G^A(E)$. $G^{R,A}(E) = g^{R,A}[E - U(t)]$ is the retarded and advanced Green function, respectively, and we express them as the adiabatic modulation of the unperturbed Green functions, $g^{R,A}(E) = (E - H \pm i\Gamma)^{-1}$ for given level broadening $\Gamma = 25$ meV. Because the zeroth order term is irrelevant to the spin pumping currents, we omit it and obtain the lesser Green function up to the first order as

$$\delta G^<(t, t) = -\frac{1}{i\hbar} \int dE \left(\frac{\partial f_0}{\partial E} \delta N(E) + f_0(E) \delta D^{(\text{sea})}(E) \right).$$

Here, δN and $\delta D^{(\text{sea})}$ are called Fermi surface and sea contributions, respectively, given by

$$\begin{aligned} \delta N(E) &= \frac{\hbar}{4\pi} [G^R \dot{U}(t) G^C - G^C \dot{U}(t) G^A], \\ \delta D^{(\text{sea})}(E) &= \frac{\hbar}{4\pi} \left[G^R \dot{U}(t) \frac{\partial G^R}{\partial E} - \frac{\partial G^R}{\partial E} \dot{U}(t) G^R + \text{h.c.} \right]. \end{aligned}$$

Usually $\delta D^{(\text{sea})}$ is considered to be small and is neglected in this work. By associating the lesser Green function and the currents of Eq. (S35), we obtain

$$\begin{aligned} j^Q(\ell) &= \frac{1}{\hbar} \text{ImTr} \int dE \frac{\partial f_0}{\partial E} \left\{ Q_{\ell, \ell} \left([\delta N(E)]^{\ell, \ell+1} H^{\ell+1, \ell} - [\delta N(E)]^{\ell, \ell-1} H^{\ell-1, \ell} \right) \right\} \\ &= -\frac{1}{a_0} \text{ImTr} \left\{ Q [\delta N(E) i v]_{E=\mu}^{\ell, \ell} \right\}, \quad T \rightarrow 0 \end{aligned} \quad (\text{S36})$$

where a_0 is a lattice constant and the velocity matrix is given by

$$v^{\ell, \ell'} = \pm \frac{ia_0}{\hbar} H^{\ell, \ell'} \delta_{\ell', \ell \pm 1}. \quad (\text{S37})$$

IV. TIGHT-BINDING MODEL

Consider a three-dimensional NM1/NM2/NM1 system of simple cubic structure (Fig. 1 in the main text). The tight-binding Hamiltonian composed of s and p orbitals is given as [3]

$$H^{(0)}(\mathbf{k}) = \begin{pmatrix} \ddots & & & & & & & & \\ & \mathcal{T}_{ll}^{(0)\dagger} & h_l^{(0)} & \mathcal{T}_{la}^{(0)} & 0 & 0 & 0 & 0 & \\ & 0 & \mathcal{T}_{la}^{(0)\dagger} & h_a^{(0)} & \mathcal{T}_{aa}^{(0)} & 0 & 0 & 0 & \\ & & & & \ddots & & & & \\ & 0 & 0 & 0 & \mathcal{T}_{aa}^{(0)\dagger} & h_a^{(0)} & \mathcal{T}_{al}^{(0)} & 0 & \\ & 0 & 0 & 0 & 0 & \mathcal{T}_{al}^{(0)\dagger} & h_l^{(0)} & \mathcal{T}_{ll}^{(0)} & \\ & & & & & & & & \ddots \end{pmatrix}, \quad (\text{S38})$$

where

$$\begin{aligned} h_i^{(0)} - \mathcal{E}_i^{(0)} &= \begin{pmatrix} 2V_{ss\sigma}^{(0)}(c_x + c_y) & 2iV_{sp\sigma}^{(0)}s_x & 2iV_{sp\sigma}^{(0)}s_y & 0 \\ -2iV_{sp\sigma}^{(0)}s_x & 2V_{pp\sigma}^{(0)}c_x + 2V_{pp\pi}^{(0)}c_y & 0 & 0 \\ -2iV_{sp\sigma}^{(0)}s_y & 0 & 2V_{pp\pi}^{(0)}c_x + 2V_{pp\sigma}^{(0)}c_y & 0 \\ 0 & 0 & 0 & 2V_{pp\pi}^{(0)}(c_x + c_y) \end{pmatrix}, \\ \mathcal{E}_i^{(0)} &= \begin{pmatrix} \epsilon_s^{(0)} & 0 & 0 & 0 \\ 0 & \epsilon_{p_x}^{(0)} & 0 & 0 \\ 0 & 0 & \epsilon_{p_y}^{(0)} & 0 \\ 0 & 0 & 0 & \epsilon_{p_z}^{(0)} \end{pmatrix}, \quad \mathcal{T}_{ij}^{(0)} = \begin{pmatrix} V_{ss\sigma}^{(0)} & 0 & 0 & V_{sp\sigma}^{(0)} \\ 0 & V_{pp\pi}^{(0)} & 0 & 0 \\ 0 & 0 & V_{pp\pi}^{(0)} & 0 \\ -V_{sp\sigma}^{(0)} & 0 & 0 & V_{pp\sigma}^{(0)} \end{pmatrix}, \end{aligned}$$

where

$$\begin{aligned}
\langle s; \mathbf{k} | h_a(t) | s; \mathbf{k} \rangle &= \epsilon_s^{(0)} + 2V_{ss\sigma}^{(0)} (\tilde{c}_x + c_y), \\
\langle p_x; \mathbf{k} | h_a(t) | p_x; \mathbf{k} \rangle &= \epsilon_{p_x}^{(0)} + 2(V_{pp\sigma}^{(0)} l_x^2 + V_{pp\pi}^{(0)} n_x^2) \tilde{c}_x + 2V_{pp\pi}^{(0)} c_y, \\
\langle p_y; \mathbf{k} | h_a(t) | p_y; \mathbf{k} \rangle &= \epsilon_{p_y}^{(0)} + 2V_{pp\pi}^{(0)} \tilde{c}_x + 2V_{pp\sigma}^{(0)} c_y, \\
\langle p_z; \mathbf{k} | h_a(t) | p_z; \mathbf{k} \rangle &= \epsilon_{p_z}^{(0)} + 2(V_{pp\sigma}^{(0)} n_x^2 + V_{pp\pi}^{(0)} l_x^2) \tilde{c}_x + 2V_{pp\pi}^{(0)} c_y, \\
\langle s; \mathbf{k} | h_a(t) | p_x; \mathbf{k} \rangle &= 2iV_{sp\sigma}^{(0)} l_x \tilde{s}_x, \\
\langle s; \mathbf{k} | h_a(t) | p_y; \mathbf{k} \rangle &= 2iV_{sp\sigma}^{(0)} s_y, \\
\langle s; \mathbf{k} | h_a(t) | p_z; \mathbf{k} \rangle &= 2iV_{sp\sigma}^{(0)} n_x \tilde{s}_x, \\
\langle p_x; \mathbf{k} | h_a(t) | p_z; \mathbf{k} \rangle &= 2(V_{pp\sigma}^{(0)} - V_{pp\pi}^{(0)}) l_x n_x \tilde{c}_x,
\end{aligned}$$

and

$$\mathcal{T}_{aa}(t) = \frac{1}{|\mathbf{d}_z(t)|^2} \begin{pmatrix} V_{ss\sigma}^{(0)} & l_z V_{sp\sigma}^{(0)} & 0 & n_z V_{sp\sigma}^{(0)} \\ -l_z V_{sp\sigma}^{(0)} & l_z^2 V_{pp\sigma}^{(0)} + n_z^2 V_{pp\pi}^{(0)} & 0 & l_z n_z (V_{pp\sigma}^{(0)} - V_{pp\pi}^{(0)}) \\ 0 & 0 & V_{pp\pi}^{(0)} & 0 \\ -n_z V_{sp\sigma}^{(0)} & l_z n_z (V_{pp\sigma}^{(0)} - V_{pp\pi}^{(0)}) & 0 & n_z^2 V_{pp\sigma}^{(0)} + l_z^2 V_{pp\pi}^{(0)} \end{pmatrix}.$$

Here, we neglect the time-dependent variation of on-site energies and assume $\epsilon_1 = \epsilon_2 = \epsilon$. Note that the strain is uniformly applied in the active region, i.e., $\partial\epsilon/\partial y = 0$. The position vectors directing nearest neighbors are

$$\begin{aligned}
\mathbf{d}_z(t) &= a_0 \hat{\mathbf{z}} [1 + \epsilon \{\cos^2 \phi \sin \omega t + \sin^2 \phi \sin(\omega t + \varphi)\}] + a_0 \hat{\mathbf{x}} \epsilon \cos \phi \sin \phi [\sin \omega t - \sin(\omega t + \varphi)], \\
\mathbf{d}_x(t) &= a_0 \hat{\mathbf{z}} \epsilon \cos \phi \sin \phi [\sin \omega t - \sin(\omega t + \varphi)] + a_0 \hat{\mathbf{x}} [1 + \epsilon \{\sin^2 \phi \sin \omega t + \cos^2 \phi \sin(\omega t + \varphi)\}],
\end{aligned}$$

and corresponding directional cosines are defined as $l_i = \hat{\mathbf{x}} \cdot \mathbf{d}_i(t) / |\mathbf{d}_i(t)|$ and $n_i = \hat{\mathbf{z}} \cdot \mathbf{d}_i(t) / |\mathbf{d}_i(t)|$ for $i = x, z$. The revised abbreviations $\tilde{c}_x \equiv \cos k_x a_0 / |\mathbf{d}_x(t)|^2$ and $\tilde{s}_x \equiv \sin k_x a_0 / |\mathbf{d}_x(t)|^2$ are used. Up to the linear order of strain ϵ ,

$$\begin{aligned}
h_a(t) - h_a^{(0)} &\approx -2\epsilon (\sin^2 \phi \sin \omega t + \cos^2 \phi \sin(\omega t + \varphi)) \begin{pmatrix} 2V_{ss\sigma}^{(0)} c_x & 2iV_{sp\sigma}^{(0)} s_x & 0 & 0 \\ -2iV_{sp\sigma}^{(0)} s_x & 2V_{pp\sigma}^{(0)} c_x & 0 & 0 \\ 0 & 0 & 2V_{pp\pi}^{(0)} c_x & 0 \\ 0 & 0 & 0 & 2V_{pp\pi}^{(0)} c_x \end{pmatrix} \\
&+ \epsilon \cos \phi \sin \phi (\sin \omega t - \sin(\omega t + \varphi)) \begin{pmatrix} 0 & 0 & 0 & 2iV_{sp\sigma}^{(0)} s_x \\ 0 & 0 & 0 & 2(V_{pp\sigma}^{(0)} - V_{pp\pi}^{(0)}) c_x \\ 0 & 0 & 0 & 0 \\ -2iV_{sp\sigma}^{(0)} s_x & 2(V_{pp\sigma}^{(0)} - V_{pp\pi}^{(0)}) c_x & 0 & 0 \end{pmatrix},
\end{aligned}$$

and

$$\begin{aligned}
\mathcal{T}_{aa}(t) - \mathcal{T}_{aa}^{(0)} &\approx -2\epsilon (\cos^2 \phi \sin \omega t + \sin^2 \phi \sin(\omega t + \varphi)) \begin{pmatrix} V_{ss\sigma}^{(0)} & 0 & 0 & V_{sp\sigma}^{(0)} \\ 0 & V_{pp\pi}^{(0)} & 0 & 0 \\ 0 & 0 & V_{pp\pi}^{(0)} & 0 \\ -V_{sp\sigma}^{(0)} & 0 & 0 & V_{pp\sigma}^{(0)} \end{pmatrix} \\
&+ \epsilon \cos \phi \sin \phi (\sin \omega t - \sin(\omega t + \varphi)) \begin{pmatrix} 0 & V_{sp\sigma}^{(0)} & 0 & 0 \\ -V_{sp\sigma}^{(0)} & 0 & 0 & V_{pp\sigma}^{(0)} - V_{pp\pi}^{(0)} \\ 0 & 0 & 0 & 0 \\ 0 & V_{pp\sigma}^{(0)} - V_{pp\pi}^{(0)} & 0 & 0 \end{pmatrix}.
\end{aligned}$$

We superpose two biaxial strains to generate lattice vibration with finite net angular momentum. One biaxial strain with $\phi_1 = 0$ and $\varphi_1 = \pi$ and the other strain with $\phi_2 = \pi/4$ and $\varphi_2 = \pi$ are overlapped where overall phase of the latter is shifted by $\pi/2$ with respect to the former. Note that the strength of each set of strains is set to $\epsilon = 0.5\%$. To obtain an insight on the perturbation we take, consider the tight-binding Hamiltonian of p orbitals in bulk simple cubic lattice. Then, the time-dependent perturbation $U^{\text{bulk}}(t)$ in the long-wavelength limit is given as

$$U^{\text{bulk}}(t) \approx -4\epsilon (V_{pp\sigma}^{(0)} - V_{pp\pi}^{(0)}) [\{L_z, L_x\} \cos \omega t - (L_z^2 - L_x^2) \sin \omega t], \quad (\text{S40})$$

which resembles $[\mathbf{L} \cdot \mathbf{u}(t)]^2$ with halved frequency for $\hat{\mathbf{u}}(t) = \hat{\mathbf{z}} \cos \omega t + \hat{\mathbf{x}} \sin \omega t$. Thus, one can conclude that the effective perturbation $[\mathbf{L} \cdot \mathbf{u}(t)]^2$ captures the lattice dynamics characterized by the circular motion of an atom about its equilibrium position, which in turn gives rise to adiabatic transformation of the OAP.

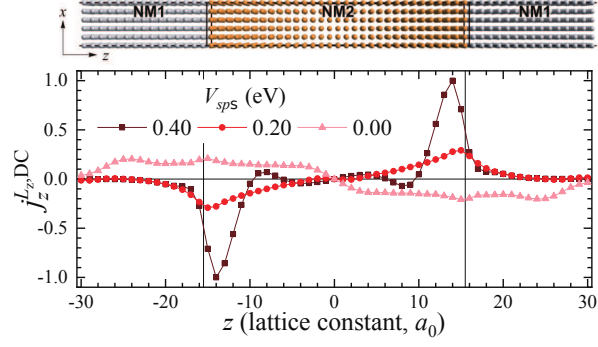


FIG. S1. Spatial profile of DC orbital pumping current driven by the time-dependent magnetic field $\mathbf{L} \cdot \mathbf{M}(t)$ for $\hat{\mathbf{M}}(t) = \hat{\mathbf{x}} \cos \omega t + \hat{\mathbf{y}} \sin \omega t$ for various strengths of sp hybridization $V_{sp\sigma}$.

V. DECAY LENGTH OF ORBITAL CURRENTS

The transmission of OAM current into adjacent layers depends on the orbital character [7]. For a given geometry, an electron propagating toward the leads experiences the crystal field which splits $|p_z\rangle$ from $|p_x\rangle$ and $|p_y\rangle$. Therefore, one can suppress the spatial oscillation of OAM response by choosing $\hat{\mathbf{M}}(t) = \hat{\mathbf{x}} \cos \omega t + \hat{\mathbf{y}} \sin \omega t$ that conveys the OAM L_z . The calculated OAM current $j_z^{L_z, DC}$ (Fig. S1) exhibits a monotonically decaying behavior rather than an oscillatory decay near the interface as illustrated in Fig. 2. Still, the OAM penetration length is not strikingly enhanced as that previously reported in ferromagnets when the orbital texture exists. Under consideration of all electrons participating in the propagation, we recognize that degenerate $|p_x\rangle$ and $|p_y\rangle$ states with nonzero in-plane wave vectors are gapped into $|p_r\rangle \equiv \cos \phi_{\mathbf{k}} |p_x\rangle + \sin \phi_{\mathbf{k}} |p_y\rangle$ and $|p_t\rangle \equiv -\sin \phi_{\mathbf{k}} |p_x\rangle + \cos \phi_{\mathbf{k}} |p_y\rangle$ by the orbital texture while the degeneracy at $\mathbf{k} = \pm k_F \hat{\mathbf{z}}$ are preserved. Note that $\phi_{\mathbf{k}} = \arg(k_x + ik_y)$ is an azimuthal angle of wave vector \mathbf{k} . As the operator $\hat{L}_z = i|p_y\rangle\langle p_x| - i|p_x\rangle\langle p_y| = i|p_t\rangle\langle p_r| - i|p_r\rangle\langle p_t|$, the broken degeneracy between $|p_r\rangle$ and $|p_t\rangle$ results in increased oscillation for states carrying L_z , and thus short-ranged orbital transport. Conversely, the overall penetration length can be extended by decreasing the strength of orbital texture as shown in Fig. S1.

VI. ORBITAL SWAPPING EFFECT

The pumped orbital current serves as a primary input of the orbital swapping effect, which is an orbital counterpart of the spin swapping effect [8–10]. Similar to the spin swapping effect which is categorized into two types, the orbital swapping effect can be classified into one that illustrates the conversion of OAM current $j_{\alpha\beta}^{\text{OAM}} \rightarrow j_{\beta\alpha}^{\text{OAM}}$ for $\alpha \neq \beta$ [Fig. S2(a)] and the other which represents the conversion of OAM current $j_{\alpha\alpha}^{\text{OAM}} \rightarrow j_{\beta\beta}^{\text{OAM}}$ for $\alpha \neq \beta$ [Fig. S2(c)]. Furthermore, we observe the swapping of OAP current $j_{\alpha\alpha\beta}^{\text{OAP}} \rightarrow j_{\gamma\beta\gamma}^{\text{OAP}}$ [Fig. S2(b)] and $j_{\alpha\beta\gamma}^{\text{OAP}} \rightarrow j_{\beta\gamma\alpha}^{\text{OAP}}$ (not shown). Note that the latter process converts AC OAP current to another AC OAP current in our model. All processes are suppressed when the orbital texture vanishes.

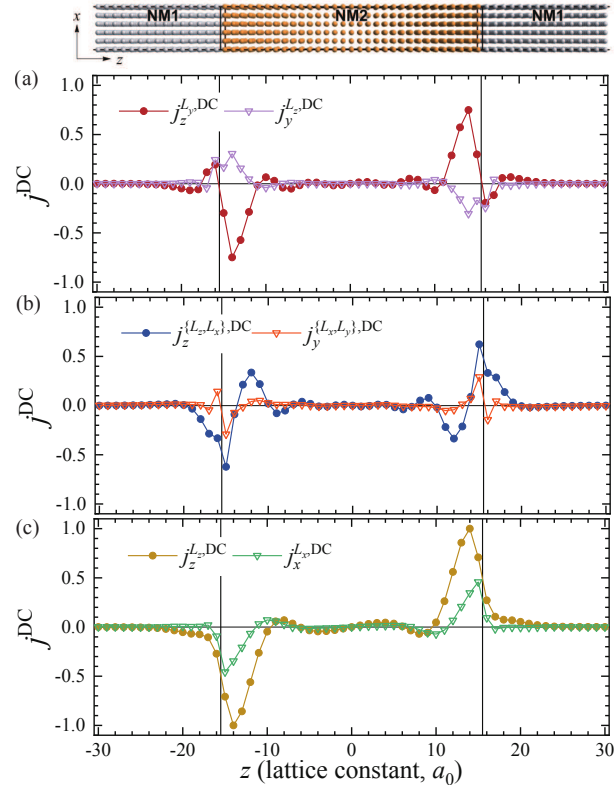


FIG. S2. Spatial profile of DC orbital pumping currents and resultant orbital swapping currents driven by the time-dependent magnetic field $\mathbf{L} \cdot \mathbf{M}(t)$ for (a,b) $\dot{\mathbf{M}}(t) = \hat{z} \cos \omega t + \hat{x} \sin \omega t$ and (c) $\dot{\mathbf{M}}(t) = \hat{x} \cos \omega t + \hat{y} \sin \omega t$.

-
- [1] K. Chen and S. Zhang, Spin Pumping in the Presence of Spin-Orbit Coupling, *Phys. Rev. Lett.* **114**, 126602 (2015).
 - [2] Y. Tserkovnyak, A. Brataas, and G. E. W. Bauer, Enhanced Gilbert Damping in Thin Ferromagnetic Films, *Phys. Rev. Lett.* **88**, 117601 (2002).
 - [3] J. C. Slater and G. F. Koster, Simplified LCAO Method for the Periodic Potential Problem, *Phys. Rev.* **94**, 1498 (1954).
 - [4] M. Luisier, A. Schenk, W. Fichtner, and G. Klimeck, Atomistic simulation of nanowires in the $sp^3d^5s^*$ tight-binding formalism: From boundary conditions to strain calculations, *Phys. Rev. B* **74**, 205323 (2006).
 - [5] S. Froyen and W. A. Harrison, Elementary prediction of linear combination of atomic orbitals matrix elements, *Phys. Rev. B* **20**, 2420 (1979).
 - [6] W. A. Harrison, *Electronic Structure and the Properties of Solids* (Freeman, San Francisco, 1980).
 - [7] D. Go, D. Jo, K.-W. Kim, S. Lee, M.-G. Kang, B.-G. Park, S. Blügel, H.-W. Lee, and Y. Mokrousov, Long-Range Orbital Torque by Momentum-Space Hotspots, *Phys. Rev. Lett.* **130**, 246701 (2023).
 - [8] M. B. Lifshits and M. I. Dyakonov, Swapping Spin Currents: Interchanging Spin and Flow Directions, *Phys. Rev. Lett.* **103**, 186601 (2009).
 - [9] S. Sadjina, A. Brataas, and A. G. Mal'shukov, Intrinsic spin swapping, *Phys. Rev. B* **85**, 115306 (2012).
 - [10] H. B. M. Saidaoui and A. Manchon, Spin-Swapping Transport and Torques in Ultrathin Magnetic Bilayers, *Phys. Rev. Lett.* **117**, 036601 (2016).